Available online at https://sej.journals.ekb.eg/
FACULTY OF ENGINEERING – SOHAG UNIVERSITY
Sohag Engineering Journal (SEJ) Vol. 4, No. 1, March 2024

Performance of Pile Group Affected by Adjacent Excavations in Sand below the Water Table

Mohamed G.I. Shaaban[a,*], Mostafa A. Abd El-Naiem[b], Abdel-Aziz A. Senoon[b], Mamdouh A. Kenawi[a]

[a]*Department of Civil Engineering, Faculty of Engineering, Sohag University, 82524, Sohag, Egypt*
[b]*Department of Civil Engineering, Faculty of Engineering, Assiut University, Assiut, Egypt*

Abstract

Numerical analysis is conducted to investigate the settlement and tilting behavior of a group of piles adjacent to an excavation in saturated sand by using PLAXIS 3D finite element software. Moreover, the analysis aims to gain a better understanding of the load transfer mechanisms of the piled foundations due to an adjacent excavation. The influences of excavation depth, pile group location from excavation, initial working load, supporting system stiffness, and stiffness of piles and cap are investigated. As excavation proceeds, settlement and tilting of the adjacent buildings can be observed at different stages of excavation. The pile group settles to its maximum amount when the rear piles are in the position of maximum greenfield ground surface settlement. The settlement of the pile group can be significantly reduced by increasing the supporting system stiffness and decreasing the pile cap's applied load. The pile group settlement due to the excavation increases from 2.99 to 3.80% of the pile diameter when the ratio of applied load to ultimate load-carrying capacity of the pile group increases from 0.25 to 0.5. A clearly noticeable tilting can be observed when the pile group is located near the excavation. By increasing the pile cap's applied load and supporting system stiffness, the pile group tilting decreases. The settlement and tilting of the pile group are almost insensitive to the modulus of elasticity of the concrete piles and the cap. Loads are transferred between the toe and the shaft of the piles at different excavation stages.

 DOI: 10.21608/sej.2024.259268.1050

Keywords: excavation; pile group; settlement; tilting; finite element analysis; load transfer; saturated sand

1. INTRODUCTION

In urban environment, most buildings are frequently constructed near to an existing one. Construction activities can affect the existing soil conditions and behavior of the adjacent structure foundations. Limited urban space in congested cities means that excavation activities are often close to existing piled structures. Excavation works can carry major risks to the nearby bridges and buildings, which are supported by pile foundations. Excavation must be carried out without causing any damage to the adjacent structures, however many cases of structural failure recently were reported [1]–[4]. The structural failures have taught us that final, temporary, and transient loading conditions must be considered during the construction process. In the United States, buildings failures due to adjacent excavation works constitute about 4% of the 225 cases of structural failures from 1989 to 2000 [5]. Reliable predictions of soil movements and the response of structures are keys to safety guarantee of the excavation and avoiding damage to the neighboring structures.

To ensure the safety of the existing pile foundations, some design charts were developed to predict the maximum lateral deformation and bending moment in the pile during the construction of the adjacent deep excavation [6]. An improved analytical method was proposed by [7] to determine the horizontal displacements, shear forces, and bending moments in an existing pile resulting from new adjacent excavation. The vast majority of previous studies concentrated on the pile lateral response to the nearby excavation. However, field investigations showed that settlement and tilting resulting from the excavation caused damage to many piled buildings [8], [9]. Extensive three-dimensional numerical analyses such as [10]–[14] and centrifuge tests such as [15], [16] were performed to illustrate the pile response and mechanisms of the load transfer in the piles nearby an excavation. Piled buildings adjacent to excavation in soft soils may exhibit several phenomena such as reduction of pile capacity, soil settlement below the pile base, relative movements between the soil and the piles,

* Corresponding author: mohamed_shabanp2@eng.sohag.edu.eg

and redistribution of load between the piles [17]. An analytical model was developed to calculate the pile settlement due to the adjacent excavation under simplified conditions [18]. Whereas the soil was presented as springs and there is no load transmission between these springs. A simplified theoretical method was proposed by [19] to predict the additional settlements and axial forces of piles due to the adjacent excavation. However, the effect of upper structures on pile settlement was not investigated. A two-stage approaches with non-linear soil-pile interaction were used by [20], [21] to evaluate the effects of ground movements induced by deep excavations on the responses of single pile and pile groups. However, these studies were limited to floating piles in a uniform ground and did not consider changes in effective stress due to the excavation. It was revealed that the vertical initial working load applied on the pile head before the excavation has a major effect on the vertical response of the pile [22]. However, the changes in the ultimate base resistance and the pile shaft normal stress were not taken into account during the excavation process in this study. Movement of soil around a loaded pile resulting from the excavation was studied by [23] using PLAXIS 3D finite element software. A two-step method was proposed to determine the response of pile-raft foundations to excavations in layered soil [24]. Although pile foundations affected by excavations and the effect of the end-bearing pile's embedment length into a stiffer deep layer were analyzed by [25], the changes in effective stress and its effect on the shaft and base resistances were not taken into account. Excavation near a bridge may result in excessive settlement of the bridge pile foundations. A three-dimensional finite element analysis was implemented by [26] to investigate the disturbance impact of a metro station excavations on nearby bridge piles. In addition, ground treatments including metro jet system treatment with different pile parameters and karst cavern treatment were evaluated to reduce the excavation disturbance on the nearby structures. In the same way, the responses of the bridge piles were measured in the field and evaluated by [27]. Results revealed that the deep excavations and water removal from sand layers both caused a soil disturbance, which accelerated settlement of the bridge piles.

A little amount of research was performed to illustrate the pile settlement in dry sandy soil due to adjacent excavation [10], [15], [28]–[30]. The reduction in pore water pressure increases the effective stress in the soil. In sandy soil, increasing the effective stress will produce considerable settlement. The water flow, introduced by the excavation influences stability of the excavation bottom and the adjacent buildings. Thus, it is necessary to investigate the ground water and its impact on soils and structures during excavation.

In engineering practice, settlement and tilting are used as performance indicators to obtain the probability of damage to structures adjacent to excavations. The settlement, tilting, and load transfer mechanisms of the loaded pile group adjacent to a supported deep excavation in saturated sand were not extensively examined. Excavation in sand below the water table may cause considerable settlement and tilting of the adjacent existing pile foundations [31], [32]. This study aimed at investigating the settlement and tilting behavior of a capped pile group adjacent to the excavations in saturated sand by varying the excavation depth, the location of the pile group from the excavation, the initial working load, the supporting system stiffness, and the stiffness of piles and cap. Furthermore, this study aimed at analyzing the load transfer mechanism and changes in the base resistance during the excavation. Also, it captured the excavation impact on the capacity and performance of the adjacent pile foundation. The results provided remarks for the design of excavation in order to prevent damage of adjacent structures.

2. THREE-DIMENSIONAL FINITE-ELEMENT ANALYSIS

Nowadays, numerical methods are the most widely used tools for geotechnical engineering applications. Therefore, the finite-element program PLAXIS 3D (CONNECT Edition V20) [33] was used in this study. The analysis was conducted to evaluate the response of a 2 x 2 pile group subjected to an initial working load and adjacent to an excavation in sand. Figure 1 shows typical excavation geometry that was selected for the analysis. The numerical analysis simulated excavations with a final depth of 15 m, a width of 20 m, and an infinite length. The excavation was supported by a 30 m depth diaphragm wall and five levels of struts. In simulation of the concrete diaphragm wall, an elastic modulus of 30 GPa was employed, and a thickness varied from 0.8 to 1.6 m. Steel pipes, having a reasonably axial rigidity of EA = 9.03 x 10^6 kN, thickness of 2.5 cm, and outer diameter of 60 cm were used as struts. The struts were spaced 8 m horizontally and 3 m vertically. The embedded length (L_p) and diameter (d_p) of the nearby piles were 12 m and 0.7 m, respectively. The bored piles were rigidly linked to the concrete pile cap. An elevated pile group was used in this investigation to avoid the soil-cap interaction and the cap's contribution in load carrying capacity. The elevated pile group represents the worst case that can happen in engineering practice. Unit weight of the concrete pile group or diaphragm wall was 25 kN/m^3. The pile cap dimensions were 3.5 m long × 3.5 m wide × 1 m deep. The concrete diaphragm wall and cap were assumed to be linear elastic behavior with Poisson’s ratio of 0.2. The pile cap was loaded by a uniformly distributed vertical load. The piles and diaphragm wall were wished-in-place, which means that behavior of pile was close to that of a bored pile and installation effects were not taken into account. Bottom-up excavation method was adopted in the current study because it is very common to use. In all stages, struts were installed 0.5 m above the excavation surface. A variety of numerical analyses were performed to investigate the response of piled buildings to an adjacent excavation.

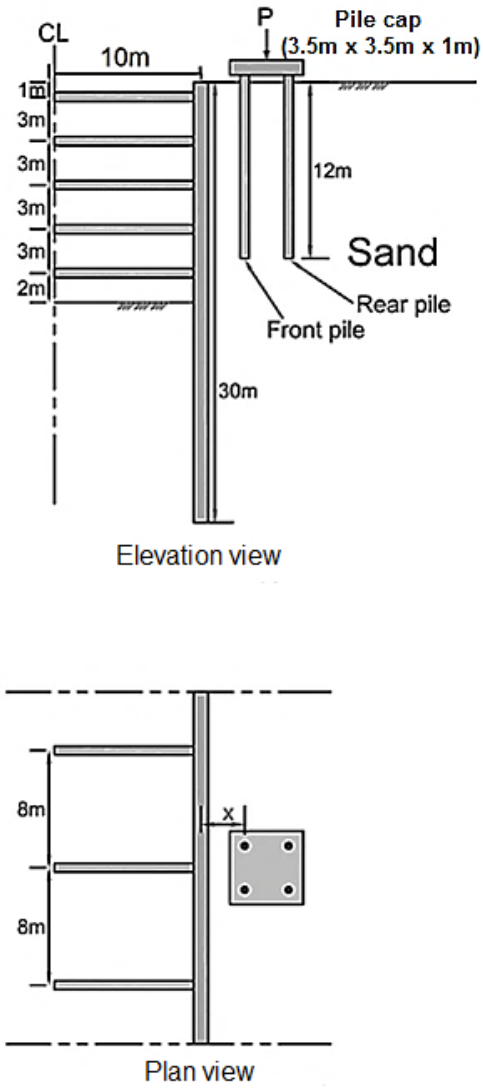

Fig. 1. Geometry of the model.

2.1. Finite Element Mesh and Boundary Conditions

A typical 3D view of the finite-element mesh and boundary conditions adopted for the current analysis is shown in Fig. 2. Only half of the excavation width was modeled because of geometrical symmetry. The mesh length in the lateral direction (y) was 70 m, as recommended by [34]. The width (x) and depth (z) of the mesh were 24 m and 45 m, respectively. The model dimensions were selected so that the boundaries were far enough away to prevent the boundary effects in the analysis. Also, model dimensions were able to capture the influence zone of the settlement trough caused by the excavations. Soil elements of the finite-element mesh were the 10-node tetrahedral elements. In addition, 6-node plate element was employed to simulate behavior of the pile cap and diaphragm wall. Moreover, 12-node interface elements were employed to simulate soil-wall interaction. The interface element has two nodes, which is compatible with the 6-noded triangular side of a plate element or soil element [33]. Struts were simulated using fixed end anchor elements. The fixed end anchors are regarded as point elements in PLAXIS 3D. Piles are usually loaded and used in a group rather than as a single pile. In this model, the center-to-center pile spacing was three times of the pile diameter. Bored piles were modeled using embedded pile with 3-node line elements. The embedded pile is represented by a beam element and interacts with the soil by means of special interface elements. A particular volume around the embedded pile based on the pile diameter (elastic zone) is assumed to make the pile almost behave like a volume pile and reducing the undesirable mesh-dependent effects. The embedded pile model is able to model the soil-pile interaction under lateral load and can reproduce behavior of a laterally loaded pile with rough shaft surface in the numerical analysis [35]. Estimation of pile group behavior by using the current embedded pile model, which is available in PLAXIS 3D was described by [36]. Moreover, the validation and formulation of the embedded pile element are available in [33], [37], [38]. These validation studies show a reasonable agreement with the calculations and field measurements for bored

piles. The skin resistance is a result of the PLAXIS calculation itself. Moreover, the maximum skin resistance can be specified in material data set of the embedded beam to avoid the undesired high values.

Normal to the vertical planes, soil deformation was restricted by roller supports. While the bottom boundary was fixed in all directions by pin supports. Whereas, the model top surface was free in all directions. Initially, level of the ground water was assumed at the ground surface, which developed a hydrostatic initial pore-water pressure profile. Free drainage was permitted at the mesh's top boundary, while the base and all vertical sides of the model were simulated as impermeable. As excavation proceeds, the water table inside the excavation was lowered to the excavation level with each stage. The excavation is sufficiently slow in this study. Therefore, the flow field will reach a steady-state situation for every excavation step. This is a reasonable assumption for rather slow excavations in high permeable soils. The water pressure on the passive side is set to zero at the excavation level and the same steady state pressure is developed on passive and active sides below the diaphragm wall. Fine mesh-size was used with a relative element size factor about (0.7). Additionally, the mesh became finer with a relative element size factor about (0.35) for the plates and embedded piles as large shear strain variations were expected. The soil elements adjacent to the excavation are fairly small and gradually increase in size as they move away from it, as shown in Fig. 2. Based on a numerical parametric analysis, mesh size was chosen under the criterion that the computed settlements have minor differences (not more than 10%) if size of the current mesh is halved. Therefore, a good balance is achieved between calculation costs and accuracy. This mesh includes 18,650 elements and 32,551 nodes with an average element size about 3.27 m.

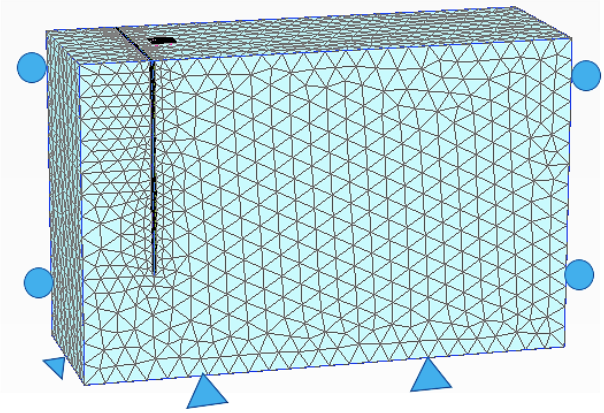

Fig. 2. Three dimensional finite-element mesh and boundary conditions adopted in the current study.

2.2. Constitutive Model and Model Parameters

Small strain characteristics of soil should be considered to better predict the ground settlement mechanism. The Hardening soil with a small-strain (HS small) model could significantly enhance the reliability of deep excavation analysis [39], [40]. Therefore, the nonlinear behavior of sand was simulated using the HS small strain soil model under drained conditions to assess the settlements on the long term. The most important features of Hardening soil with a small-strain constitutive model are taking into account the increased stiffness of soils at small strains, and considering the difference between Young's modulus values under unloading and loading conditions. Accurate modelling of small-strain nonlinearity in the soil model is very important in prediction of settlement adjacent to an excavation. The soil parameters given in Table 1 were taken from a reference solution by [39], [41]. These model and soil parameters in the HS small model were verified previously by many authors by comparing numerically simulated experimental data with real measured data. The numerical data resembled reasonably well the measured data. Validation and verification of the HS small model are available in [39]. The value of interface strength reduction factor (R_{inter}= 0.95) gives a plausible simulation of sand deformations [38].

TABLE 1. SOIL PARAMETERS USED IN THE FINITE ELEMENT ANALYSES.

γ_{sat} (kN/m^3)	C′ (kN/m^2)	Φ′ (°)	ν_{ur}	E_{50}^{ref} (kN/m^2)	E_{oed}^{ref} (kN/m^2)	E_{ur}^{ref} (kN/m^2)	m	$\gamma_{0.7}$	G_0^{ref} (kN/m^2)	P_{ref} (kN/m^2)
20.0	1.0	35.0	0.20	45000	45000	180000	0.55	0.0002	168750	100

Note: γ_{sat} = saturated unit weight; C′ = effective cohesion; Φ′ = effective friction angle; ν_{ur} = Poisson's ratio; E_{50}^{ref} = triaxial compression stiffness; E_{oed}^{ref} = primary oedometer stiffness; E_{ur}^{ref} = unloading/reloading stiffness; m = power for stress-level dependency of stiffness; $\gamma_{0.7}$ = shear strain at which Gs = 0.722G_0; G_0^{ref} = shear modulus at very small strains; P_{ref} = reference stress for stiffness.

2.3. Numerical Modelling Procedure

Staged construction provides an accurate simulation of various loading, construction and excavation processes. For the purpose of this research, the numerical modeling procedures are summarized as follows:

1. Establish the initial stresses and boundary conditions with K_o procedure.
2. Active the pile cap and the four embedded piles (wished-in-place pile group).
3. Apply an initial vertical working load on the pile cap.
4. Active the wished-in-place diaphragm wall.
5. Simulate excavation by deactivating soil elements from the ground surface to level -1.5 m.
6. Install struts at level -1.0 m.
7. Excavate down to level -4.5 m.
8. Install struts at level -4.0 m.
9. Excavate down to level -7.5 m.
10. Install struts at level -7.0 m.
11. Excavate down to level -10.5 m.
12. Install struts at level -10.0 m.
13. Excavate down to level -13.5 m.
14. Install struts at level -13.0 m.
15. Excavate down to level -15.0 m.

3. NUMERICAL ANALYSIS AND VERIFICATION CASE STUDY

This section presents the numerical modeling of a case study and compares between the observed readings and model results. An actual full-scale instrumented investigation was presented by [42] to study the response of an existing pile due to an adjacent excavation. Figure 3 displays the soil profile and parameters estimated from nearby boreholes. In the site, the original ground water table existed at about 4 m below the ground surface. The general layout of the case study is presented in Fig. 4. A diaphragm wall with 0.8 m thick and 31 m long was used to support this excavation. The diameter and embedded length of the pile were 1.0 m and 46 m, respectively. An in-pile inclinometer was installed in the pile to monitor its behavior during excavation. The Hardening soil with a small-strain (HS small) model is the most applicable option to simulate the soil's nonlinear behavior [38]–[41]. The parameters for (HS small) model of soil layers were obtained from the widely used empirical values of [43].

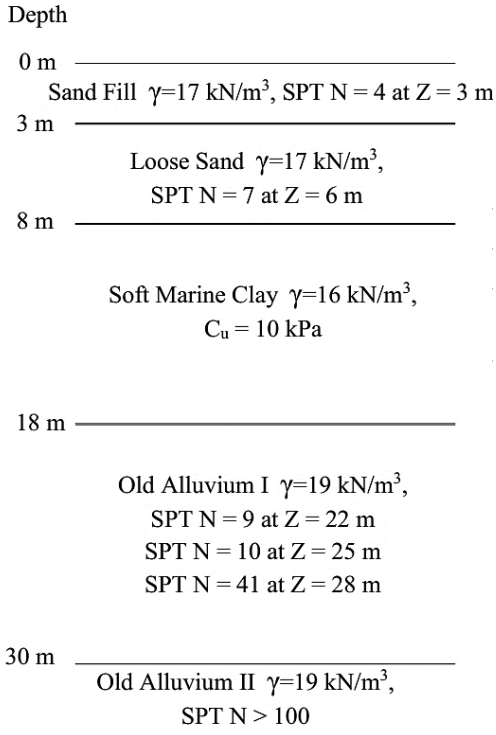

Fig. 3. Soil profile and parameters [42].

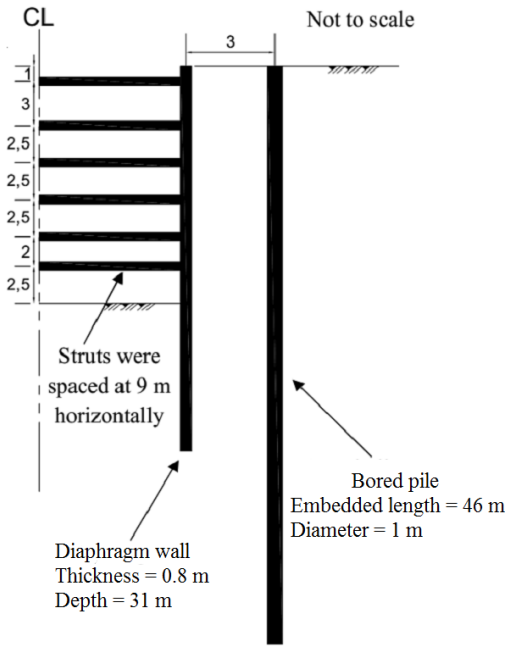

Fig. 4. Cross section through the excavation, all dimensions in m [42].

Figure 5 presents the measured and computed lateral movement and bending moment for the bored pile at the end of the 16 m excavation. This figure shows that the computed lateral movement and bending moment of the pile reasonably match with the measured results, in both the magnitude and the profiles. Although the computed lateral deflection is slightly smaller at the pile head, general trends similar to those seen can be recorded. Thus, the good match demonstrates the ability of the software, (HS small) model, and embedded pile model to predict the pile response.

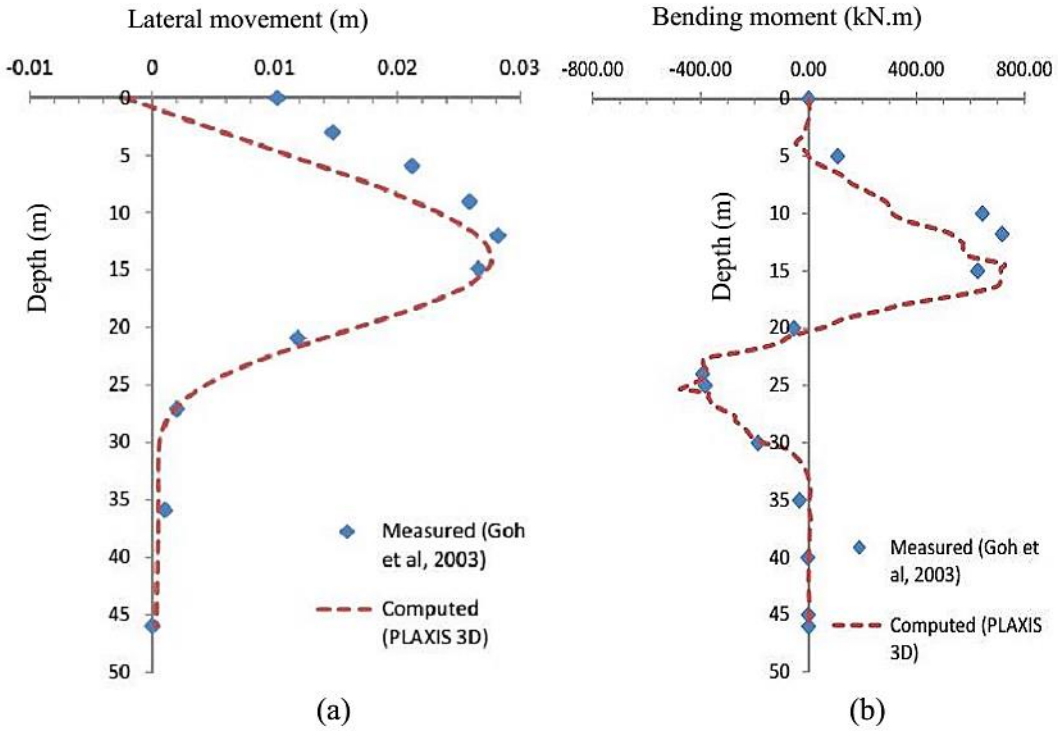

Fig. 5. Comparison of computed and measured pile response (a) pile lateral movements and (b) bending moment along the pile length at the end of the 16 m excavation.

4. ANALYSIS OF RESULTS

4.1. Determination of the Axial Load Carrying Capacity of the Pile Group

The vertical response of the pile is significantly affected by the vertical initial working load applied on the pile head before the excavation [22]. Thus, it is required to calculate the load-carrying capacity of the pile group before the excavation. Figure 6 shows the load-settlement curve, which was obtained by performing numerical simulation of the pile load test before the excavation commencement. The ultimate load-carrying capacity of the pile group (i.e., failure load) was determined to be 8293 kN, according to the failure criterion proposed by [44] for large diameter bored piles. This failure criterion is expressed as follows:

$$\Delta_{\mathrm{ph,max}} = 0.045 d_p + \frac{1}{2}\frac{P_h L_p}{A_p E_p} \quad (1)$$

where $\Delta_{ph,max}$ is the maximum pile head settlement which defines the ultimate load, d_p is the pile diameter, P_h is the pile head load, L_p is the pile length, A_p is the cross-sectional area of the pile, and E_p is the elastic modulus of pile. With a safety factor of 2.5, the working load is determined to be 3317 kN. A pile group settlement of 0.63% of pile diameter was noted because of the applied working load.

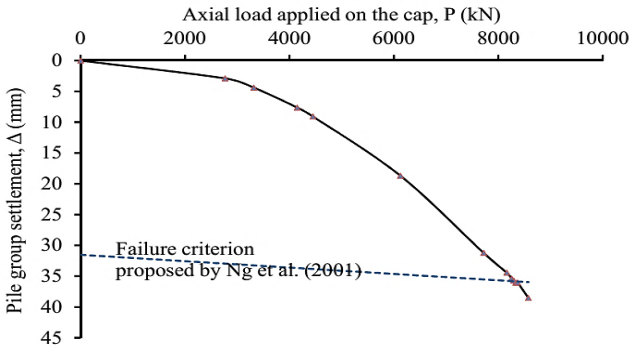

Fig. 6. Load-settlement relation before excavation.

4.2. Development of Ground Surface Settlement

An excavation with a final depth of 15 m was simulated in the numerical analysis. The excavation was supported by a 1.0 m thick diaphragm wall and five levels of struts. Figure 7 represents the ground surface settlement resulting from the adjacent excavation for the greenfield case at different excavation depths. The greenfield settlement is referred to the settlement with absence of piles and building. It can be observed that type of settlement profile caused by this excavation is concave type, in which maximum surface settlement happens at a distance away from the wall. This type is due to installation of struts in the wall, especially in the wall upper part [45]. Distance between the diaphragm wall and location of the maximum ground surface settlement is in range from 0.5 to 0.6 of the excavation depth. As expected, ground surface settlement is significantly increased with increasing the excavation depth. The location of the maximum ground surface settlement is near to the excavation in the case of shallow excavation, then the distance between the maximum settlement point and the excavation gradually increases with the increase in the excavation depth. Indeed, the maximum ground surface settlement reaches 20.2 mm and occurs at a distance of 9 m from the wall after completing the excavation (i.e., He = 15 m). The results presented in Fig. 7 are consistent with those in [10], [29], [34], indicating that the numerical results are reasonable. It is important to keep the pavement in a good condition. The effect of maintenance activities on the environment was also introduced as a third objective by [46].

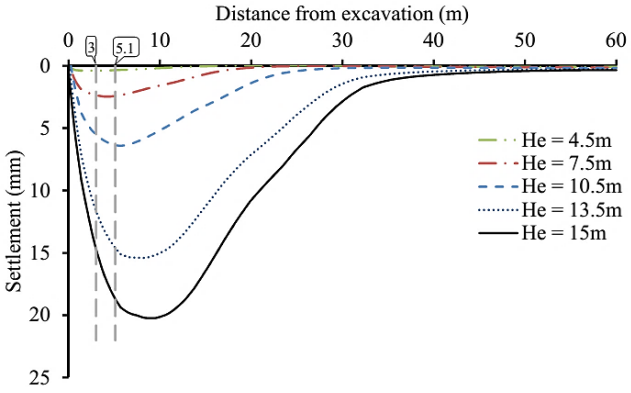

Fig. 7. Greenfield ground surface settlement due to excavation.

4.3. Effects of Excavation Depth

Figure 8 shows settlement of the pile group with the advancement of the excavation. The pile group settlement (Δ) and excavation depth (He) are normalized by the pile diameter (d_p) and pile length (L_p), respectively. The normalized settlement of the pile group is presented in percentage. For the results given in this section, the front piles are located 3 m away from the 1.0 m thick diaphragm wall. The load on the pile cap before excavation is 3317 kN. The pile group is simulated using an elastic modulus of 30 GPa. Displacement is set to zero before construction of the excavation. Hence, settlement due to initial working loads and diaphragm wall installation are not included in the presented results to exclude deformations before excavation. Pile group settlement is evaluated at the center of the pile cap with reference to its original elevation. Wall penetration depth does not significantly affect the behavior of the wall and the adjacent soil [47]. In addition, increasing the penetration depth of the wall could not contribute to property protection and does not affect the wall deformations as long as the retaining wall is stable [34]. Therefore, results with the same wall depth at different excavation depths could be compared. It is thus concluded that, increasing of excavation depth leads to increasing settlement of the pile group. A Similar observation was noted by [10], [29] but the amounts of settlement are different. This is attributed to the increase in soil movements and stress relief with excavation advancement. A significant pile group settlement is observed where the excavation level is closer to level of the pile toe due to the end bearing resistance loss. In addition, deeper excavation ($He/L_p > 1.0$) gives a faster rate of increase in pile group settlement due to the significant loss of the end bearing resistance. During the last 4.5 m excavation, settlement of the pile group increases almost linearly with increase of the excavation depth. The pile group settlement due to the initial applied working load is 0.63% d_p. At the end of the 15 m excavation, the pile group settlement is 3.44% d_p. Therefore, the settlement of the pile group because of initial applied working load and final excavation is about 4.07% d_p. The damage limit of maximum settlement for building supported by pile foundations in sand is 51 mm [48]. A factor of safety may be considered; this gives a safety limit of 38 mm. In addition, the maximum allowable settlement is (5.1% d_p) based on the failure criterion proposed by [44].

The pile capacity is often determined from a load-settlement curve and the induced settlement can be considered as an extra load on the head of the pile. The pile group acts as if it is axially loaded by an equivalent load of 7372 KN on the pile cap because of this additional settlement (based on the load-settlement curve shown in Fig. 6). Consequently, the pile group capacity decreased by 49% of the pile group ultimate capacity due to the excavation. However, the pile group ultimate capacity is not physically decreased due to the excavation. It indicates instead that the serviceability limit state of the pile is broken due to the nearby excavation. In other words, safety factor for the pile group is decreased from 2.5 to 1.13 due to the excavation. The significant decrease of safety factor indicates a potential serviceability issue for pile foundations nearby the excavations.

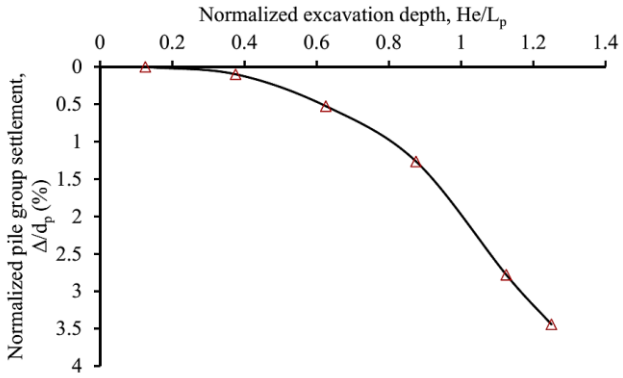

Fig. 8. Effect of excavation depth on pile group settlement.

Figure 9 shows tilting of the pile cap with the excavation advancement. The tilting is presented in percentage and it is estimated by the differential settlement between two edges of the pile cap divided by the horizontal distance between them. Tilting toward the excavation is considered to be positive and tilting away from the excavation is considered to be negative. In other words, positive tilting takes place when piles in the front row settle more than piles in the rear row and negative tilting takes place when piles in the rear row settle more than piles in the front row. An unexpected trend of pile cap tilting is found. Initially tilting is positive and increases with excavation depth till the excavation depth to pile length ratio 0.6. Further advancement of excavation induces negative pile cap tilting. This tilting trend can be explained by a closer look at the greenfield ground surface settlement (concave type settlement), which is presented in Fig. 7. If the pile group is located between the wall and location of the maximum ground surface settlement, pile group tilts away from the excavation (negative tilting) and the rear piles experience higher soil movements. On the contrary, the presence of the pile group at larger distance from the excavation provides a pile cap tilting toward the excavation (positive tilting). It was found that, although the pile cap tilts, the magnitude of this tilting is very small in the cases of ($He/L_p < 0.875$). However, the maximum tilting of the pile cap is 0.1% in the case of (He = 15 m). Although this value is well within the tilting limit of 0.2% for buildings [48], [49], tilt becomes clearly noticeable. Moreover, tilting causes additional bending moments in beams and floor slabs due to the eccentricity of the building weight.

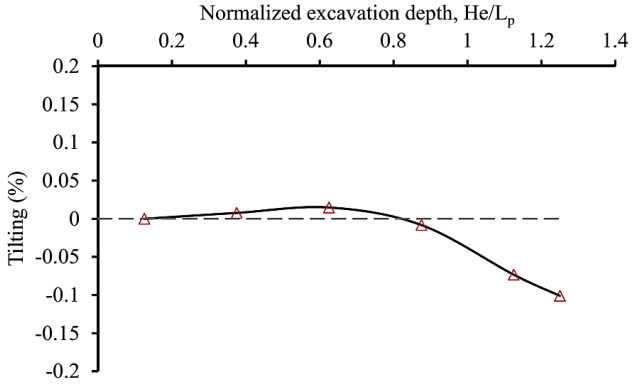

Fig. 9. Effect of excavation depth on pile cap tilting.

4.4. Impacts of Pile Group Location from Excavation

The effect of pile group distance from the excavation on the pile group settlement and tilting are investigated by varying value of the distance from 3 to 37.5 m. To give a better insight in the effects of pile group distance from the excavation, the normalized pile group settlement corresponding to front pile distance from the excavation (X) is given in Fig. 10. For simplicity, only the results after the excavation depth reaches 10.5 m, 13.5 m, and 15 m are included in the figure. These results are for a pile group with a vertical load of 3317 kN and an elastic modulus of 30 GPa. The excavation is supported by a multi-strutted wall with a thickness of 1.0 m. It appears that excavation has a very minor effect on settlement of nearby pile group when the distance from excavation exceeds 2 He, which proposed that the main influence zone of the excavation on the adjacent pile group is about twice the excavation depth. Initially, 3.56. A similar trend of ground surface settlement is observed during the excavation in greenfield conditions, see Fig. 7. It can be inferred that the settlements of the pile group and the greenfield ground surface settlement are relevant to each other. In addition, maximum settlement is induced when the rear

piles are located in zone of the maximum greenfield ground surface settlement at the end of final excavation (i.e., He = 15 m). The effect of pile group distance from excavation on the pile cap tilting is shown in Fig. 11 by varying value of the distance from 3 to 37.5 m. When the pile group is situated closer to the excavation, it experiences maximum tilting. This observation is in a line with the results by [13], although their analyses were performed in soft clay. There is no tilting when the excavation is carried out at 10.5 m from the front pile (X/He = 0.7). After finishing the excavation, pile cap tilts away from the excavation in all cases with (X < 10.5 m). On the contrary, when excavation takes place at (X > 10.5 m), pile cap tilts toward the excavation after completing the excavation. Excavation at 3 m from the front pile induces a relatively large settlement and the most critical case in terms of tilting among all cases in this study. Thus, the distance between the front pile and wall was taken as 3 m in the present analyses of excavation impacts on a pile group.

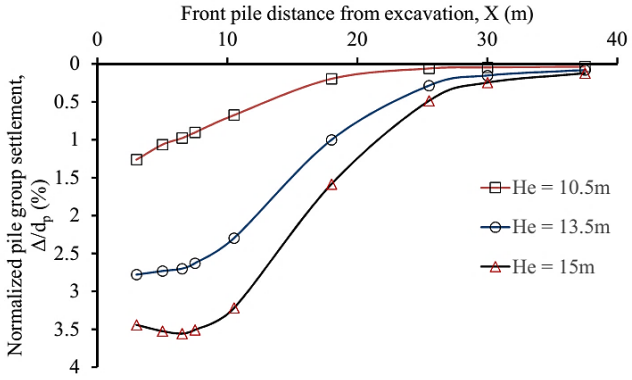

Fig. 10. Effect of pile group location on settlement of the pile group.

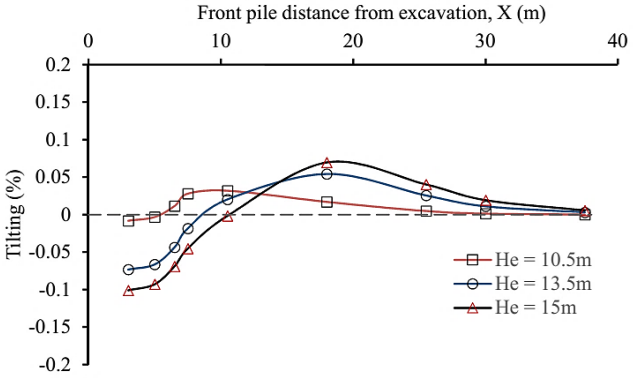

Fig. 11. Effect of pile group location on tilting of the pile cap.

4.5. Impacts of Initial Vertical Working Load

Figure 12 presents the influence of initial working load on the pile group settlement due to the excavation. The load is normalized by the ultimate load-carrying capacity of the pile group (P_u). The model is analyzed with various working load in order to investigate its influence. The settlement due to applied load before the excavation commencement is also plotted in Fig. 12 for comparison purposes. For this case, an existing pile group with an elastic modulus of 30 GPa is located at 3.0 m away from the 1.0 m thick diaphragm wall. Data presented in Fig. 12 clearly indicate that the loaded pile group settles significantly more than the unloaded pile group when subjected to a similar adjacent excavation. Obviously, settlement of the pile group increases almost linearly with increase in the working load. This is probably due to the reduction of skin resistance and soil stiffness underneath the pile toe and around the pile shaft. This shows that the induced settlement is highly dependent on the working load. Thus, the presence of working load would tend to produce noticeable additional settlement of the existing pile group. When there is zero working load on the pile cap, the pile group settlement is about 2.32% of the pile diameter after completing the excavation (i.e., He = 15 m). Moreover, when the working load varies from 0.25 P_u to 0.5 P_u, the pile group settlement increases from 2.99 to 3.80% of d_p after completing the excavation.

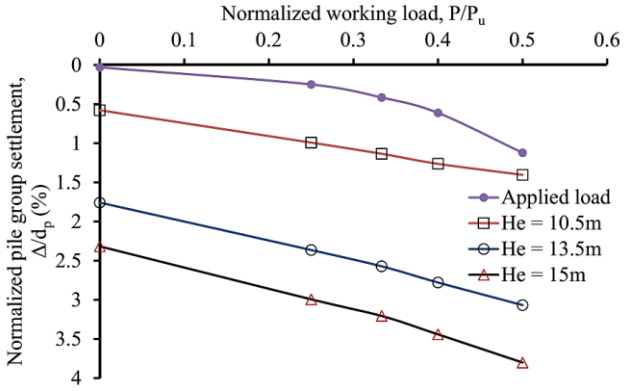

Fig. 12. Effect of initial working load on pile group settlement.

The pile cap tilting is plotted against the normalized working load in Fig. 13. Tilting for each case is smaller than 0.12% and it is seen to decrease with increase in the working load. Based on the computed results, it can be noted that increase in working load from zero to 0.5 P_u causes a small decrease in tilting of the pile cap at the end of the 15 m excavation (from 0.12 to 0.09%). This is because applying a high distributed load on the pile cap attempts to force the piled structures to settle uniformly. Moreover, in the case of zero applied load, magnitudes of tilting are 0.02%, 0.09%, and 0.12% after excavation depth reaches 10.5 m, 13.5 m, and 15 m, respectively.

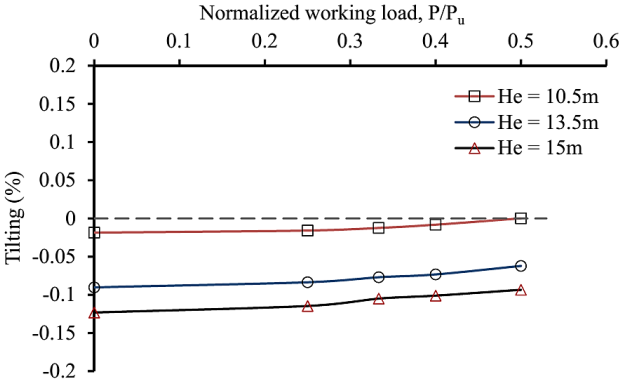

Fig. 13. Effect of initial working load on pile cap tilting.

4.6. Impacts of Supporting System Stiffness

The pile group settlement, as a function of system stiffness factor (K), is shown in Fig. 14. Stiffness of the supporting system is represented by system stiffness factor (K) in this research. This system stiffness factor (K) was defined by [50] as follows:

$$K = \frac{E_w I_w}{\gamma_{water} S_v^4} \quad (2)$$

where $E_w$is the elastic modulus of wall, I_w is the moment of inertia per unit length of wall, γ_{water} is the unit weight of water, and S_v is the vertical distance between struts. Influence of stiffness of the supporting system is studied by varying the wall thickness. Four different values of the wall thickness ranging from 0.8 to 1.6 m are considered. For these results, front piles are located at 3.0 m away from the diaphragm wall, which has an elastic modulus of 30 GPa. Initial applied load on the pile cap before excavation is 3317 kN. As would be expected, stiffness of the wall is a very important parameter for the settlement amount. Settlement of the pile group continuously decreases with increasing the wall stiffness. In addition, the larger the wall stiffness, the smaller is the tilting, as shown in Fig. 15. This can be attributed to the smaller soil movements with increased stiffness of the supporting system. The design methodology suggested by [51] to reduce ground movements associated with the excavation is also justified these findings. When the wall thickness is 0.8 m (i.e., K = 1580.25), the settlement of the pile group due to initial applied working load and final excavation is about 5.13% d_p, which slightly exceeds the maximum allowable settlement (5.1% d_p) based on [44].

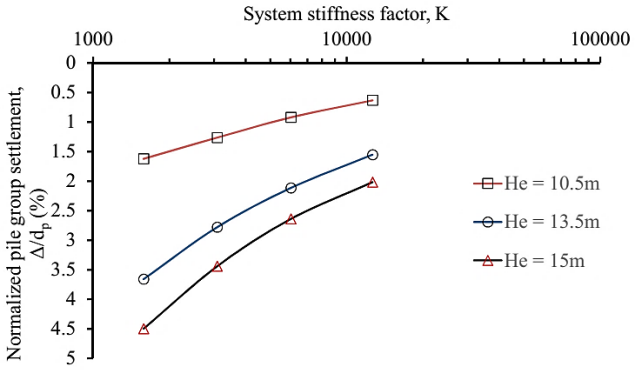

Fig. 14. Effect of support system stiffness on pile group settlement.

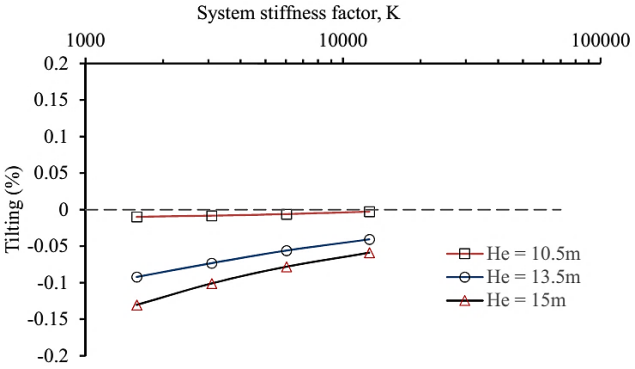

Fig. 15. Effect of support system stiffness on pile cap tilting.

4.7. Impacts of Stiffness of Piles and Cap

Figure 16 shows the effect of stiffness of piles and cap on settlement. The effect of stiffness of piles and cap on pile cap tilting is presented in Fig. 17. In order to examine the stiffness effect, three different modulus of elasticity of the piles and cap ranging from 20 to 40 Gpa are considered. For the results presented in Figs. 16 and 17, pile groups are located at 3.0 m away from the 1.0 m thick diaphragm wall. The pile cap is subjected to a 3317 kN initial load. The results indicate that pile group settlement and tilting due to adjacent excavation are not sensitive to the concrete modulus of elasticity of the pile group. This is because soil movements resulting from the excavation do not depend on the concrete modulus of elasticity of the pile group. In reality, the pile group responses are greatly affected by stiffness of soil [52].

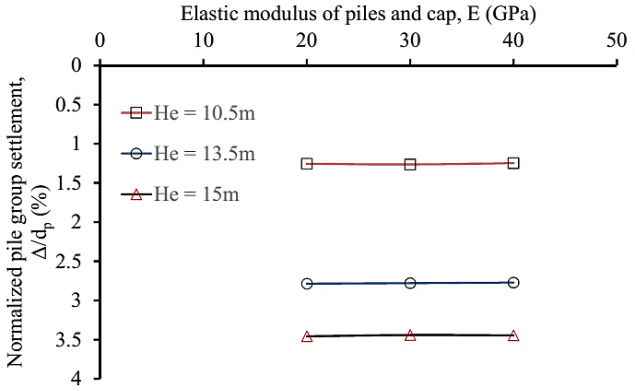

Fig. 16. Effect of stiffness of the piles and cap on pile group settlement.

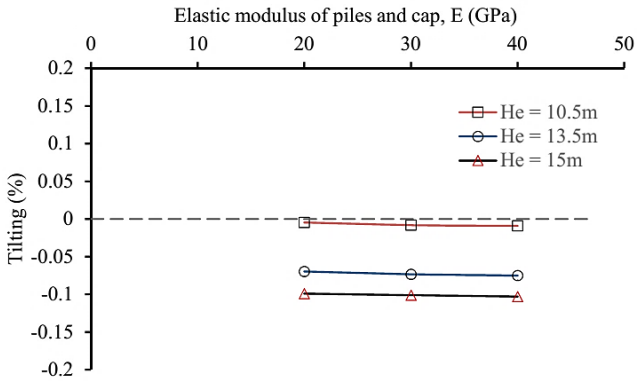

Fig. 17. Effect of stiffness of the piles and cap on pile cap tilting.

4.8. Load Transfer Mechanism

The load transfer mechanisms for a pile must be taken into account to ensure the integrity of structures and foundations. In order to better demonstrate the mechanisms of the load transfer, axial load distribution and changes in pile group base resistance before and during the excavation are discussed in this section.

4.8.1 Axial load distribution along the depth of the pile

Figure 18 shows the computed distribution of axial load along the piles before and during the excavation. For reference, axial force in the piles due to the initial applied load before excavation is also shown in the figure. Results indicate that axial load distribution is generally similar in shape for each case, including the position of maximum axial force, but the magnitude of the axial force is different. The maximum axial forces are found at head of the piles. The general trends in the figure indicate that no negative skin resistance is developed; however, the skin resistance is affected by the adjacent excavation. This could be attributed to the change in horizontal pressure acting on the pile shaft with the excavation advancement. This figure demonstrates that deep excavation causes a stress relief and soil movements. Moreover, the axial force along the front pile and rear pile induced by excavation are different. After excavating to 10.5 m depth, axial force decreases in the front pile and increases in the rear pile. However, axial force at the pile toe decreases in both front pile and rear pile due to the stress relief at the end of the 15 m excavation.

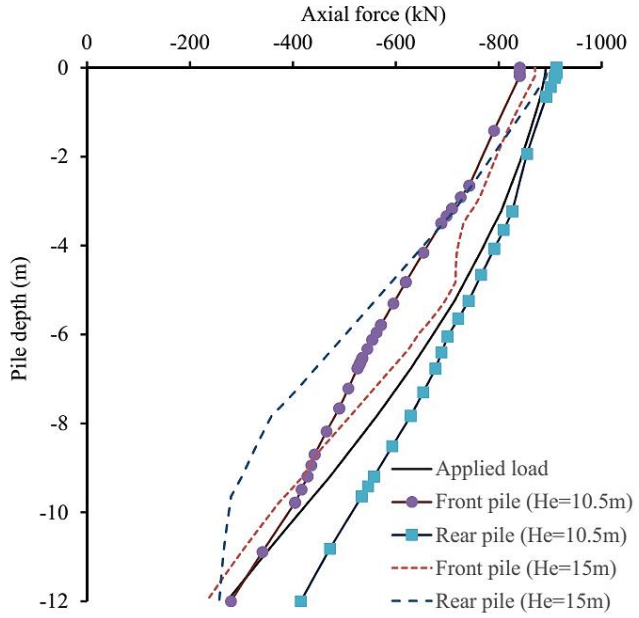

Fig. 18. Axial force distribution along the pile shaft before and during the excavation.

4.8.2 Pile group base resistance during excavation

To explore the pile group base resistance during the excavation process, changes in the base resistance for different excavation depths are presented in Fig. 19. The base resistance is normalized by the vertical applied load on the pile cap. Results suggest that the end-bearing resistance and shaft resistance of the pile are changed due to the adjacent excavation. Initially, there is a transfer of the load from shaft to toe, which introduces an increase in pile base resistance till ($He/L_p = 0.875$) and then a reduction in the pile base resistance occurs due to load transfer from toe to shaft. This observation is due to end bearing resistance loss at deeper excavation. The maximum and minimum base resistance of the pile group are found to be 47% and 32.6% of the vertical load on the pile cap, respectively. Before commencement of the excavation, the pile carried approximately 67.4% of the working load by its shaft resistance and the remainder by its end-bearing resistance. If the pile length is higher than the excavation depth, any pile deformation increases the base resistance (until the maximum is reached), because reduction of the shaft friction is balanced by the additional base resistance.

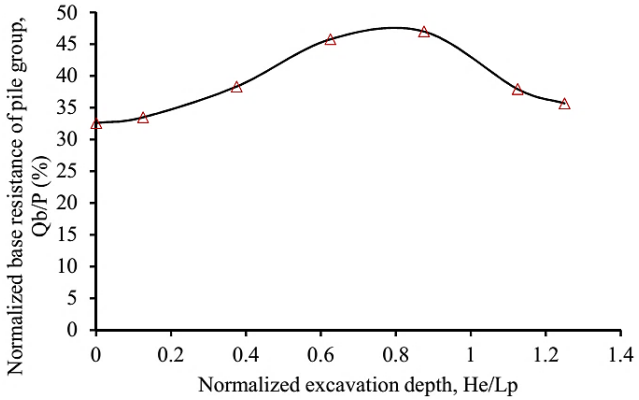

Fig. 19. Effect of excavation depth on base resistance of pile group.

5. CONCLUSIONS AND RECOMMENDATIONS

This study described the pile group behavior due to the ground deformations caused by the adjacent excavation. The problem was numerically investigated by performing three-dimensional finite element parametric analyses. The following main conclusions can be drawn from the computed results:

1. Settlement at the center of the pile cap increases with excavation depth and, in general, is not affected by stiffness of the piles or the cap. The settlement of the pile group can significantly be reduced by increasing the supporting system stiffness and decreasing the working load on the pile cap. This is because soil movements resulting from the excavation decrease rapidly as the supporting system stiffness increases and the excavation depth decreases. In addition, soil stiffness underneath the pile toe and around the pile shaft reduces with the advancement of excavation.
2. A large settlement of the pile group is noted where the excavation level is closer to level of the pile toe due to the end bearing resistance loss. Moreover, the presence of the rear piles at the zone of maximum greenfield ground surface settlement provides the most critical scenario in terms of settlement. The main influence zone of excavation on the adjacent pile group is about twice the excavation depth.
3. Deeper excavation gives a clearly noticeable tilting. The pile cap tilts toward the excavation in the cases with high pile distance from excavation, but tilts away from the excavation when it is located closer to the excavation. In addition, when the pile group is located near the excavation, it experiences maximum tilting. Moreover, the larger supporting system stiffness, the smaller is the tilting.
4. An increase in the working load from zero to 0.5 P_u (ultimate load-carrying capacity of the pile group) causes a small decrease in tilting of the pile cap after completing the excavation. This is because applying a high distributed load on the pile cap attempts to force the piled structures to settle uniformly. Moreover, the pile cap tilting is not affected by stiffness of piles and cap.
5. During the excavation, there is a transfer of the load from shaft to toe till ($He/L_p = 0.875$), and then a transfer of the load from toe to shaft. This is because the reduction in shaft friction is counterbalanced by the additional base resistance during the shallow excavation, but the base resistance reduces at deeper excavation. Thus, the end-bearing resistance and the shaft resistance of the pile are changed due to the adjacent excavation after finishing the excavation. Moreover, the axial force along the front pile and rear pile induced by excavation are different.

In this study, all the numerical analyses of deep underwater excavation works are performed on sandy soils to verify the effect of excavation on the adjacent four-pile group. Any extrapolation from these findings needs to be done with caution.

Funding

No funding was received for conducting this study.

Declaration of interests

The authors have no relevant financial or non-financial interests to disclose.

References

[1] W.-D. Wang, C. W. W. Ng, Y. Hong, Y. Hu, and Q. Li, "Forensic study on the collapse of a high-rise building in Shanghai: 3D centrifuge and numerical modelling," *Géotechnique*, vol. 69, no. 10, pp. 847–862, 2019.

[2] W. Wang, Q. Li, and Y. Hu, "Collapse of a high-rise building with pretensioned high-strength concrete piles," *Proc. Inst. Civ. Eng. - Forensic Eng.*, vol. 173, no. 1, pp. 3–12, Feb. 2020, doi: 10.1680/jfoen.19.00012.

[3] J. Chai, S. Shen, W. Ding, H. Zhu, and J. Carter, "Numerical investigation of the failure of a building in Shanghai, China," *Comput. Geotech.*, vol. 55, pp. 482–493, Jan. 2014, doi: 10.1016/j.compgeo.2013.10.001.

[4] W. D. Wang, Q. Li, Y. Hu, J. W. Shi, and C. W. W. Ng, "Field Investigation of Collapse of a 13-Story High-Rise Residential Building in Shanghai," *J. Perform. Constr. Facil.*, vol. 31, no. 4, p. 04017012, Aug. 2017, doi: 10.1061/(ASCE)CF.1943-5509.0001005.

[5] K. Wardhana and F. C. Hadipriono, "Study of Recent Building Failures in the United States," *J. Perform. Constr. Facil.*, vol. 17, no. 3, pp. 151–158, Aug. 2003, doi: 10.1061/(ASCE)0887-3828(2003)17:3(151).

[6] D. S. Liyanapathirana and R. Nishanthan, "Influence of deep excavation induced ground movements on adjacent piles," *Tunn. Undergr. Sp. Technol.*, vol. 52, pp. 168–181, Feb. 2016, doi: 10.1016/j.tust.2015.11.019.

[7] J. Liu, C. Shi, C. Cao, M. Lei, and Z. Wang, "Improved analytical method for pile response due to foundation pit excavation," *Comput. Geotech.*, vol. 123, p. 103609, Jul. 2020, doi: 10.1016/j.compgeo.2020.103609.

[8] M. Korff, *Response of piled buildings to the construction of deep excavations*, vol. 13. IOS Press, 2013.

[9] H. G. Poulos, "THE INFLUENCE OF CONSTRUCTION'SIDE EFFECTS' ON EXISTING PILE FOUNDATIONS," *Geotech. Eng.*, vol. 36, no. 1, pp. 51–68, 2005.

[10] J. Shi, J. Wei, C. W. W. Ng, and H. Lu, "Stress transfer mechanisms and settlement of a floating pile due to adjacent multi-propped deep excavation in dry sand," *Comput. Geotech.*, vol. 116, p. 103216, Dec. 2019, doi: 10.1016/j.compgeo.2019.103216.

[11] D. A. Mangnejo and N. Mangi, "The Responses of an End-Bearing Pile to Adjacent Multipropped Excavation: 3D Numerical Modelling," *Civ. Eng. J.*, vol. 5, no. 3, p. 552, Mar. 2019, doi: 10.28991/cej-2019-03091267.

[12] M. A. Soomro, D. A. Mangnejo, R. Bhanbhro, N. A. Memon, and M. A. Memon, "3D finite element analysis of pile responses to adjacent excavation in soft clay: Effects of different excavation depths systems relative to a floating pile," *Tunn. Undergr. Sp. Technol.*, vol. 86, pp. 138–155, Apr. 2019, doi: 10.1016/j.tust.2019.01.012.

[13] M. Shakeel and C. W. W. Ng, "Settlement and load transfer mechanism of a pile group adjacent to a deep excavation in soft clay," *Comput. Geotech.*, vol. 96, pp. 55–72, Apr. 2018, doi: 10.1016/j.compgeo.2017.10.010.

[14] M. A. Soomro, A. S. Brohi, M. A. Soomro, D. K. Bangwar, and S. A. Bhatti, "3D Numerical Modeling of Pile Group Responses to Excavation-Induced Stress Release in Silty Clay," *Eng. Technol. Appl. Sci. Res.*, vol. 8, no. 1, pp. 2577–2584, Feb. 2018, doi: 10.48084/etasr.1748.

[15] C. W. W. Ng, J. Wei, H. Poulos, and H. Liu, "Effects of Multipropped Excavation on an Adjacent Floating Pile," *J. Geotech. Geoenvironmental Eng.*, vol. 143, no. 7, p. 04017021, Jul. 2017, doi: 10.1061/(ASCE)GT.1943-5606.0001696.

[16] C. F. Leung, J. K. Lim, R. F. Shen, and Y. K. Chow, "Behavior of Pile Groups Subject to Excavation-Induced Soil Movement," *J. Geotech. Geoenvironmental Eng.*, vol. 129, no. 1, pp. 58–65, Jan. 2003, doi: 10.1061/(ASCE)1090-0241(2003)129:1(58).

[17] M. Korff and R. J. Mair, "Response of piled buildings to deep excavations in soft soils," in *Proceedings of the 18th International Conference on Soil Mechanics and Geotechnical Engineering, Paris*, 2013, pp. 2035–2039.

[18] M. Korff, R. J. Mair, and F. A. F. Van Tol, "Pile-Soil Interaction and Settlement Effects Induced by Deep Excavations," *J. Geotech. Geoenvironmental Eng.*, vol. 142, no. 8, p. 04016034, Aug. 2016, doi: 10.1061/(ASCE)GT.1943-5606.0001434.

[19] Y.-Y. Liang, N.-W. Liu, F. Yu, X.-N. Gong, and Y.-T. Chen, "Prediction of Response of Existing Building Piles to Adjacent Deep Excavation in Soft Clay," *Adv. Civ. Eng.*, vol. 2019, pp. 1–11, Dec. 2019, doi: 10.1155/2019/8914708.

[20] A. Franza, A. M. Marshall, and R. Jimenez, "Non-linear soil–pile interaction induced by ground settlements: pile displacements and internal forces," *Géotechnique*, vol. 71, no. 3, pp. 239–249, 2021.

[21] C. Zheng, A. Franza, and R. Jimenez, "A prediction method based on elasticity and soil-structure interaction for deep-excavation induced deformations of pile foundations," in *Challenges and Innovations in Geomechanics: Proceedings of the 16th International Conference of IACMAG-Volume 2 16*, 2021, pp. 239–246.

[22] R. Zhang, J. Zheng, H. Pu, and L. Zhang, "Analysis of excavation-induced responses of loaded pile foundations considering unloading effect," *Tunn. Undergr. Sp. Technol.*, vol. 26, no. 2, pp. 320–335, Mar. 2011, doi: 10.1016/j.tust.2010.11.003.

[23] N. Liu, J. Yu, X. Gong, and Y. Chen, "Analysis of soil movement around a loaded pile induced by deep excavation," *IOP Conf. Ser. Earth Environ. Sci.*, vol. 189, no. 3, p. 032053, Nov. 2018, doi: 10.1088/1755-1315/189/3/032053.

[24] L. Mu, W. Chen, M. Huang, and Q. Lu, "Hybrid Method for Predicting the Response of a Pile-Raft Foundation to Adjacent Braced Excavation," *Int. J. Geomech.*, vol. 20, no. 4, p. 04020026, Apr. 2020, doi: 10.1061/(ASCE)GM.1943-5622.0001627.

[25] C. Zheng, A. Franza, and R. Jimenez, "Analysis of floating and end-bearing pile foundations affected by deep-excavations," *Comput. Geotech.*, vol. 153, p. 105075, 2023.

[26] Y. Yang, J. Li, C. Liu, J. Ma, S. Zheng, and W. Chen, "Influence of deep excavation on adjacent bridge piles considering underlying karst cavern: a case history and numerical investigation," *Acta Geotech.*, vol. 17, no. 2, pp. 545–562, 2022.

[27] Y. Yang *et al.*, "Performance of a deep excavation and the influence on adjacent piles: A case history in karst region covered by clay and sand," *Undergr. Sp.*, vol. 8, pp. 45–60, 2023.

[28] M. A. Soomro, N. Mangi, W.-C. Cheng, and D. A. Mangnejo, "The Effects of Multipropped Deep Excavation-Induced Ground Movements on Adjacent High-Rise Building Founded on Piled Raft in Sand," *Adv. Civ. Eng.*, vol. 2020, pp. 1–12, Oct. 2020, doi: 10.1155/2020/8897507.

[29] C. W. W. Ng, M. Shakeel, J. Wei, and S. Lin, "Performance of Existing Piled Raft and Pile Group due to Adjacent Multipropped Excavation: 3D Centrifuge and Numerical Modeling," *J. Geotech. Geoenvironmental Eng.*, vol. 147, no. 4, p. 4021012, Apr. 2021, doi: 10.1061/(ASCE)GT.1943-5606.0002501.

[30] H. Karira, A. Kumar, T. H. Ali, D. A. Mangnejo, and N. Mangi, "A parametric study of settlement and load transfer mechanism of piled raft due to adjacent excavation using 3D finite element analysis," *Geomech. Eng.*, vol. 30, no. 2, pp. 169–185, 2022, doi: 10.12989/gae.2022.30.2.169.

[31] Y. Liu, B. Xiang, and M. Fu, "Influence of Dewatering in Deep Excavation on Adjacent Pile Considering Water Insulation Effect of Retaining Structures," *Geotech. Geol. Eng.*, vol. 37, no. 6, pp. 5123–5130, 2019.

[32] Y. Tan and Y. Lu, "Forensic diagnosis of a leaking accident during excavation," *J. Perform. Constr. Facil.*, vol. 31, no. 5, p. 04017061, 2017.

[33] R. B. J. Brinkgreve, L. Zampich, and N. R. Manoj, "PLAXIS 3D CONNECT Edition V20 tutorial manual," *Delft Univ. Technol. PLAXIS bv, Netherlands*, 2019.

[34] C.-Y. Ou, *Deep excavation: theory and practice*. CRC Press, 2006.

[35] T. P. T. Dao, "Validation of PLAXIS embedded piles for lateral loading (M. Sc. Thesis)," 2011.

[36] H. K. Engin, E. G. Septanika, and R. B. J. Brinkgreve, "Estimation of pile group behavior using embedded piles," in *Proceeding of the 12th International Conference of International Association for Computer Methods and Advances in Geomechanics, Goa, India*, 2008, pp. 3231–3238.

[37] F. Tschuchnigg and H. F. Schweiger, "The embedded pile concept – Verification of an efficient tool for modelling complex deep foundations," *Comput. Geotech.*, vol. 63, pp. 244–254, Jan. 2015, doi: 10.1016/j.compgeo.2014.09.008.

[38] I. Al-abboodi and T. T. Sabbagh, "Numerical Modelling of Passively Loaded Pile Groups," *Geotech. Geol. Eng.*, vol. 37, no. 4, pp. 2747–2761, Aug. 2019, doi: 10.1007/s10706-018-00791-z.

[39] T. Benz, "Small-strain stiffness of soils and its numerical consequences (Ph. D. Thesis)," Stuttgart, Inst. f. Geotechnik., 2007.

[40] Y.-M. Hsieh, P. H. Dang, and H.-D. Lin, "How Small Strain Stiffness and Yield Surface Affect Undrained Excavation Predictions," *Int. J. Geomech.*, vol. 17, no. 3, p. 04016071, Mar. 2017, doi: 10.1061/(ASCE)GM.1943-5622.0000753.

[41] H. F. Schweiger, "Results from numerical benchmark exercises in geotechnics," in *Proc. 5th European Conf. Numerical Methods in Geotechnical Engineering (P. Mestat, ed.), Presses Ponts et chaussees, Paris*, 2002, pp. 305–314.

[42] A. T. C. Goh, K. S. Wong, C. I. Teh, and D. Wen, "Pile Response Adjacent to Braced Excavation," *J. Geotech. Geoenvironmental Eng.*, vol. 129, no. 4, pp. 383–386, Apr. 2003, doi: 10.1061/(ASCE)1090-0241(2003)129:4(383).

[43] F. Xuan, "Behavior of diaphragm walls in clays and reliability analysis. M. Eng," Thesis, Nanyang Technological University, Singapore, 2009.

[44] C. W. W. Ng, T. L. Y. Yau, J. H. M. Li, and W. H. Tang, "New Failure Load Criterion for Large Diameter Bored Piles in Weathered Geomaterials," *J. Geotech. Geoenvironmental Eng.*, vol. 127, no. 6, pp. 488–498, Jun. 2001, doi: 10.1061/(ASCE)1090-0241(2001)127:6(488).

[45] P.-G. Hsieh and C.-Y. Ou, "Shape of ground surface settlement profiles caused by excavation," *Can. Geotech. J.*, vol. 35, no. 6, pp. 1004–1017, 1998.

[46] A. S. Mohamed, T. A. Abdel-Wahed, and A. M. Othman, "Investigating effective maintenance policies for urban networks of residential cities by using optimum and sensitivity analyses," *Can. J. Civ. Eng.*, vol. 47, no. 6, pp. 691–703, 2020.

[47] L. Zdravkovic, D. M. Potts, and H. D. St John, "Modelling of a 3D excavation in finite element analysis," *Géotechnique*, vol. 55, no. 7, pp. 497–513, Sep. 2005, doi: 10.1680/geot.2005.55.7.497.

[48] A. W. Skempton and D. H. MacDonald, "The allowable settlements of buildings.," *Proc. Inst. Civ. Eng.*, vol. 5, no. 6, pp. 727–768, 1956.

[49] L. M. Zhang and A. M. Y. Ng, "Probabilistic limiting tolerable displacements for serviceability limit state design of foundations," *Géotechnique*, vol. 55, no. 2, pp. 151–161, Mar. 2005, doi: 10.1680/geot.55.2.151.59527.

[50] G. W. Clough, E. M. Smith, and B. P. Sweeney, "Movement control of excavation support systems by iterative design," in *Foundation engineering: Current principles and practices*, 1989, pp. 869–884.

[51] L. S. Bryson and D. G. Zapata-Medina, "Method for estimating system stiffness for excavation support walls," *J. Geotech. Geoenvironmental Eng.*, vol. 138, no. 9, pp. 1104–1115, 2012.

[52] H. G. Poulos, "Pile group settlement estimation—Research to practice," *Found. Anal. Des. Innov. Methods*, pp. 1–22, 2006.